Modulational instability oscillation in nonlinear dispersive ring cavity

Masataka Nakazawa and Kazunori Suzuki
NTT Transmission Systems Laboratories, Optical Communication Laboratory, Tokai, Ibaraki-ken 319-11, Japan

Hermann A. Haus
Electrical Engineering and Computer Science and Research Laboratory of Electronics, Massachusetts Institute of Technology, Cambridge, Massachusetts 02139

(Received 16 May 1988)

Periodic-intensity self-oscillation caused by modulational instability is observed for the first time in a nonlinear dispersive fiber ring cavity. The oscillation stops immediately when the phase coherence is disturbed by cavity detuning. It is found that a noninstantaneous response of the nonlinear index competes with the modulational instability gain and produces asymmetrical Stokes sidebands.

Modulational instability (MI) is a general feature of wave propagation in nonlinear dispersive media and has been studied in such diverse fields as fluid dynamics, nonlinear optics, and plasma physics.[1,2] It refers to a process in which weak perturbations from the steady state grow exponentially as a result of an interplay between nonlinearity (self-phase-modulation) and group velocity dispersion (GVD).

In optical fibers, MI is responsible for the break-up into solitons[3,4] of cw optical excitation. In 1980, Hasegawa and Brinkman proposed a new coherent infrared source by means of MI, in which a coherent signal is generated by extracting the sideband of the MI spectrum.[5] Tai *et al.* have recently reported observation of this phenomenon.[6] Induced modulational instability, which can be achieved by applying a weak external field, has also been theoretically and experimentally investigated.[7,8] The effects of fiber loss, the envelope time derivative, and the cross phase modulation on MI have been studied by several authors.[9–12]

It is well known that a ring cavity filled with a nonlinear dielectric medium and subjected to intense light exhibits instabilities and chaos.[13–17] When the GVD of the nonlinear medium is negligibly small, the system can be described as an Ikeda instability, where a nonlinear phase shift of the order of π is crucial.[13,15] When one incorporates GVD; i.e., in the case of solitons in the ring cavity, it has been theoretically shown that instability and chaos are also observed as the pump power increases.[16,17]

In this paper we show that a new type of a periodic intensity oscillation occurs through the MI in a nonlinear dispersive fiber ring cavity. The physical mechanism behind the instability oscillation is one of periodic feedback into the nonlinear dispersive cavity, in which the MI gain can compensate for the loss in the cavity, resulting in a steady-state self-oscillation. Since the MI oscillation (MIO) has a wide generality in nonlinear systems, one may apply it to a plasma or fluid to generate very high-intensity plasma or fluid-pulse trains.[1,2,14]

The experimental setup for the MIO is shown in Fig. 1, which a nonlinear ring cavity is constructed with a single-mode fiber. The pump source is a 100-MHz mode-locked color-center laser at a 1.5-μm region. After passing through an isolator, the pump pulse is coupled into a ring cavity through a beam splitter. As the pump pulse propagates down the fiber, the small MI builds up from the self-phase-modulation noise. The output from the fiber is reflected at the movable corner cube, and then the pump with the small modulational instability is fed back (in part) into the ring cavity to "seed" the pulse breakup. If the pump is synchronized to the succeeding pump pulse, the MI is amplified coherently in the cavity, and eventually steady-state MI oscillation takes place. When proper synchronization is achieved, the sideband signals become large, whereas they collapse when the phase coherence is disturbed. A $\lambda/4$ plate is inserted into the cavity to change the coupling efficiency to the next loop.

The MI gain of the Stokes field amplitude, g_{MI}, is given by[3,6]

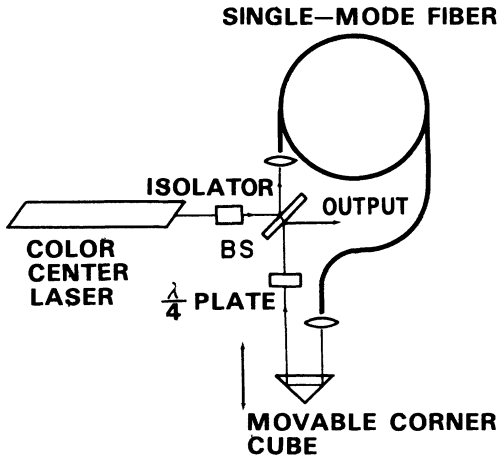

FIG. 1. Experimental setup for observation of modulational instability oscillation.

$$g_{\mathrm{MI}}=\frac{|k''|\Omega^2}{2}\left[\frac{2\omega n_2|E|^2}{c|k''|\Omega^2}-1\right]^{1/2}. \tag{1}$$

Here, n_2 is the nonlinear index coefficient, k'' the group velocity dispersion (equal to $\partial^2 k/\partial\omega^2$), c the speed of light, and E the field amplitude of the pump wave. The maximum gain is achieved at $\Omega_{\max}$ $(=2\pi f_{\max})$

$$\Omega_{\max}=\left[\frac{\omega}{c}\left|\frac{n_2}{k''}E^2\right|\right]^{1/2} \tag{2}$$

and is given by

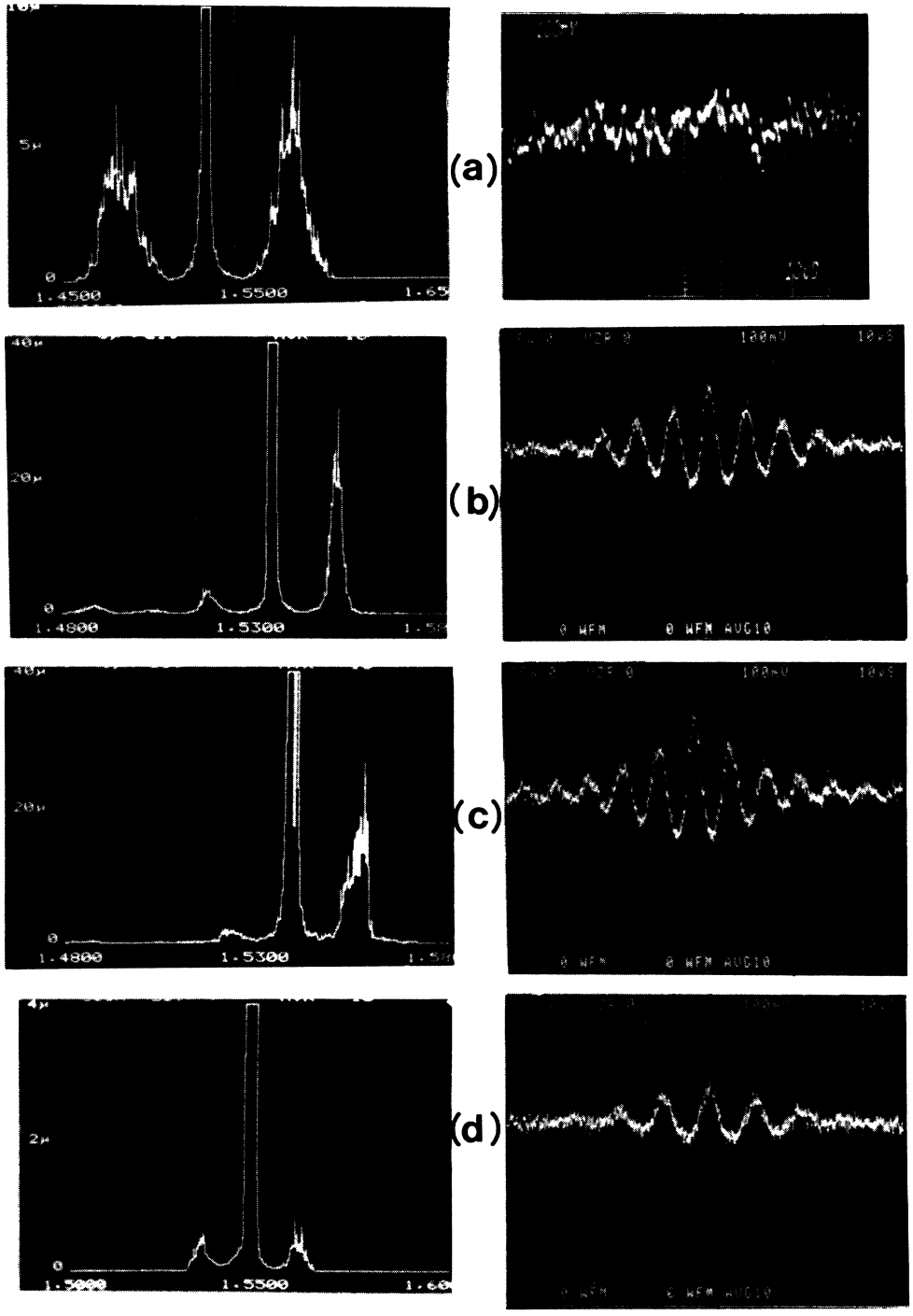

FIG. 2. Pump-wavelength dependence the oscillation waveforms and spectra of the MIO. (a)–(d) correspond to pump wavelengths of 1.525, 1.535, 1.540, and 1.550 μm, respectively. Spectra are on the left-hand side and the corresponding autocorrelation waveforms are on the right-hand side. One division of the autocorrelation waveforms corresponds to 0.5 ps.

$$g_{\max}=\tfrac{1}{2}n_2\frac{\omega}{c}\mid E\mid^2 . \tag{3}$$

If we take an example of the pump peak power coupled into the cavity $I_p=20$ W, $n_2=3.2\times10^{-16}$ cm^2/W for silica, $A_{\text{eff}}=5\times10^{-7}$ cm^2, and $\lambda=1.55$ μm, the amplitude coefficient of the MI gain $g_{\max}$ becomes as high as 2.6×10^{-2} (1/m).

For the self-induced Raman gain, Gordon, Mitschke, and Mollenauer have pointed out that the noninstantaneous response of the nonlinear index is essentially the same phenomenon as the Raman gain.[18,19] Thus one may suppose that the index change Δn follows[20]

$$\frac{\partial\Delta n}{\partial t}=-\frac{\Delta n}{T}+\frac{n_2 I}{T} \tag{4}$$

and the solution is

$$\Delta n=\frac{n_2 I}{1-i\Omega T}=\frac{n_2 I}{1+(\Omega T)^2}(1+i\Omega T) , \tag{5}$$

where Ω is the modulation frequency and T is a relaxation time constant of $\Delta n(t)$. Thus Δn is complex, and there is gain for $\Omega<0$ on the low-frequency side (the Stokes field is amplified) and loss for $\Omega>0$ on the high-frequency side (the anti-Stokes field is absorbed). The Raman gain of the Stokes amplitude peaks at $\Omega T=1$, and is given as

$$g_{\text{Raman}}=I_m\{\Delta n\}k_0 =\tfrac{1}{2}n_2\frac{\omega}{c}\mid E\mid^2 . \tag{6}$$

Comparing Eq. (6) with Eq. (3), the growth rate of the MI is the same as that of the Raman gain at the frequency offset such that $\Omega T=1$. At smaller frequency offsets the MI gain dominates.

The oscillation waveforms and spectra of MIO are shown in Fig. 2, where the fiber length was 100 m and the pump wavelength was varied from 1.525 μm (zero GVD) to 1.550 μm (negative GVD). For the parametric process in pulsed operation, the temporal overlap among the Stokes, the anti-Stokes, and the pump pulses is important to achieve a large gain. Since the Stokes shift is a few 10 nm to a 1.5-μm region, the walk-off becomes 10–30 ps/km, which means that the effective interaction length is approximately equal to the ring-cavity length of 100–300 m for a pump-pulse width of 13 ps. Figures 2(a)–2(d) correspond to pump wavelengths of 1.525, 1.535, 1.540, and 1.550 μm, respectively. The pump power for each wavelength was 45, 42, 40, and 39 W, respectively. It is apparent that the MIO takes place when the pump wavelength is in the negative GVD region. There was no parametric process when the pump wavelength was set in the positive GVD region ($\lambda=1.510$ μm, $k''=0.94$ ps^2/km). Parametric four-photon mixing is observed at zero dispersion ($k''=0.01$ ps^2/km), the Stokes and the anti-Stokes wavelengths of which are $\lambda_S=1.569$ μm and $\lambda_{AS}=1.481$ μm. Although the sidebands are generated, no modulational instability was observed as seen in the autocorrelation trace, Fig. 2(a). When the pump wavelength is slightly shifted to the negative GVD ($\lambda=1.530$ μm, $k''=-0.31$ ps^2/km), small MI oscillations began to be observed. As the pump wavelength is extended toward larger wavelengths as shown in Figs. 2(b)–2(d), clear MIO can be seen. Here, some asymmetry is observed between the Stokes and the anti-Stokes signals, where k'' values for Figs. 2(b)–2(d) were -0.64, -0.96, and -1.63 ps^2/km, respectively. In addition, as we expected from Eq. (2), the period of the MIO decreases with an increase of the pump wavelength (increase of k''), the results of which are plotted in Figs. 3(a)–3(b).

It can be said that the asymmetric sideband is generated by competition between the MI gain and the Raman gain. As we discussed, the Raman gain becomes large when the period of the MI (corresponding to soliton width) is short. This means that the asymmetry can be enhanced when Ω is large, that is, the pump wavelength is set near the zero dispersion region. This can be experimentally confirmed in Figs. 2(b)–2(d). However, this asymmetry becomes small in Fig. 2(d) by setting the pump wavelength to 1.550 μm. The oscillation period of the MIO becomes long at 1.550 μm, so that the Raman gain can be reduced and the MI gain becomes dominant. This phenomenon corresponds to removing the self-frequency shift for soliton propagation by extending the input pulse width, which means that the nonlinear index can respond instantaneously.

Output characteristics of the MIO are summarized in Figs. 3(a)–3(d). $f_{\max}$ and the modulation period changes, as a function of wavelength, are shown in Fig. 3(a). The open circles are experimental data for $f_{\max}$ and the closed circles for the modulation period. The solid and dashed lines are theoretical curves given by Eq. (3), where

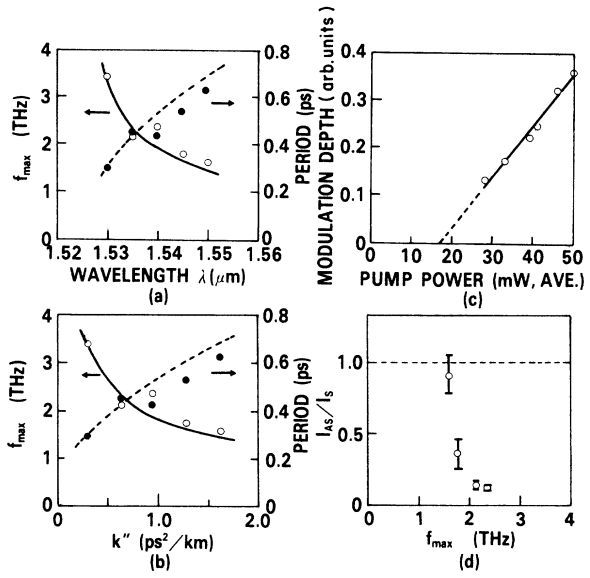

FIG. 3. Output characteristics of the MIO. (a) $f_{\max}$ and the modulation period changes as a function of pump wavelength, (b) $f_{\max}$ and the modulation period changes as a function of k'', (c) threshold and output (modulation depth) vs average pump power for fiber length of 250 m, and (d) asymmetry change between I_{AS} and I_S as a function of pump wavelength.

a fiber core diameter of 10 μm and a pump peak power of 42 W are used for the calculation. It is shown that these agree well. For example, the calculated f_{max} at 1.535 μm is 2.35 THz, which is in good agreement with the experimental value of 2.13 THz. A small deviation from the estimation is due to the difference of the coupled power for each wavelength and to the fact that the pump is not actually a continuous wave, but a pulse. Figure 3(a) is redrawn in Fig. 3(b) as a function of k''.

The threshold characteristics at $\lambda = 1.545$ μm are shown in Fig. 3(c), where the fiber length was extended to 250 m. The modulation depth, measured at the center of the autocorrelation trace, increases linearly with an increase of pump power coupled into the fiber. There is no doubt that the system has a clear threshold level, and the average pump power of the threshold was 17.5 mW, corresponding to the pump peak power of 13.5 W. The ratio of the anti-Stokes to Stokes intensities, defined I_{AS}/I_S, is described in Fig. 3(d) as a function of the pump wavelength. For large f_{max}, the response of the index change becomes noninstantaneous, so that the Raman gain builds up and the asymmetry is enhanced. It was also found that the MIO stopped for cavity detunings of ± 1 mm, where there was no apparent change in period of the MIO for the cavity detunings; i.e., Ω was fixed.

In our experiments, the pump power required for generation of the $N=1$ soliton is of the order of 10 mW and the soliton period is longer than 50 km because of the broad pump width (13 ps) and small GVD (-1 ps/km nm). However, the pump power that we used in the experiment was about 40 W, which is 4×10^3 times larger than the $N=1$ soliton power. Thus, we may say that the MI on the soliton pulse is equivalent to effective excitation of very-high-order solitons by synchronous pumping. It has not been made clear yet experimentally if the instabilities and chaos occur for the pump power corresponding to $N=2$–5.[17]

The authors would like to express their thanks to Y. Kimura for fruitful discussion, and to M. Ohashi and N. Kuwaki for supplying dispersion-shifted fibers.

[1]T. B. Benjamin and J. E. Feir, J. Fluid Mech. **27**, 417 (1967).
[2]A. Hasegawa, *Plasma Instabilities and Nonlinear Effects* (Springer-Verlag, Heidelberg, 1975).
[3]A. Hasegawa and F. Tappert, Appl. Phys. Lett. **23**, 142 (1973).
[4]L. F. Mollenauer, R. H. Stolen, and J. P. Gordon, Phys. Rev. Lett. **45**, 1095 (1980).
[5]A. Hasegawa and W. F. Brinkman, IEEE J. Quantum Electron. **16**, 694 (1980).
[6]K. Tai, A. Hasegawa, and A. Tomita, Phys. Rev. Lett. **56**, 135 (1986).
[7]A. Hasegawa, Opt. Lett. **9**, 288 (1984).
[8]K. Tai, A. Tomita, J. L. Jewell, and A. Hasegawa, Appl. Phys. Lett. **49**, 236 (1986).
[9]D. Anderson and M. Liask, Opt. Lett. **9**, 468 (1984).
[10]P. K. Shukla and J. J. Rasmussen, Opt. Lett. **11**, 171 (1986).
[11]M. J. Potasek and G. P. Agrawal, Phys. Rev. A **36**, 3862 (1987).
[12]G. P. Agrawal, Phys. Rev. Lett. **59**, 880 (1987).
[13]K. Ikeda, Opt. Commun. **30**, 257 (1979).
[14]H. M. Gibbs, *Optical Bistability: Controlling Light with Light* (Academic, New York, 1985).
[15]H. Nakatsuka, S. Asaka, H. Itoh, K. Ikeda, and M. Matsuoka, Phys. Rev. Lett. **50**, 109 (1984).
[16]K. Nozaki and N. Bekki, Phys. Rev. Lett. **50**,1226 (1983).
[17]K. J. Blow and N. J. Doran, Phys. Rev. Lett. **52**, 526 (1984).
[18]J. P. Gordon, Opt. Lett. **11**, 662 (1986).
[19]F. M. Mitschke and L. F. Mollenauer, Opt. Lett. **11**, 659 (1986).
[20]H. A. Haus and M. Nakazawa, J. Opt. Soc. Am. B **4**, 652 (1987).

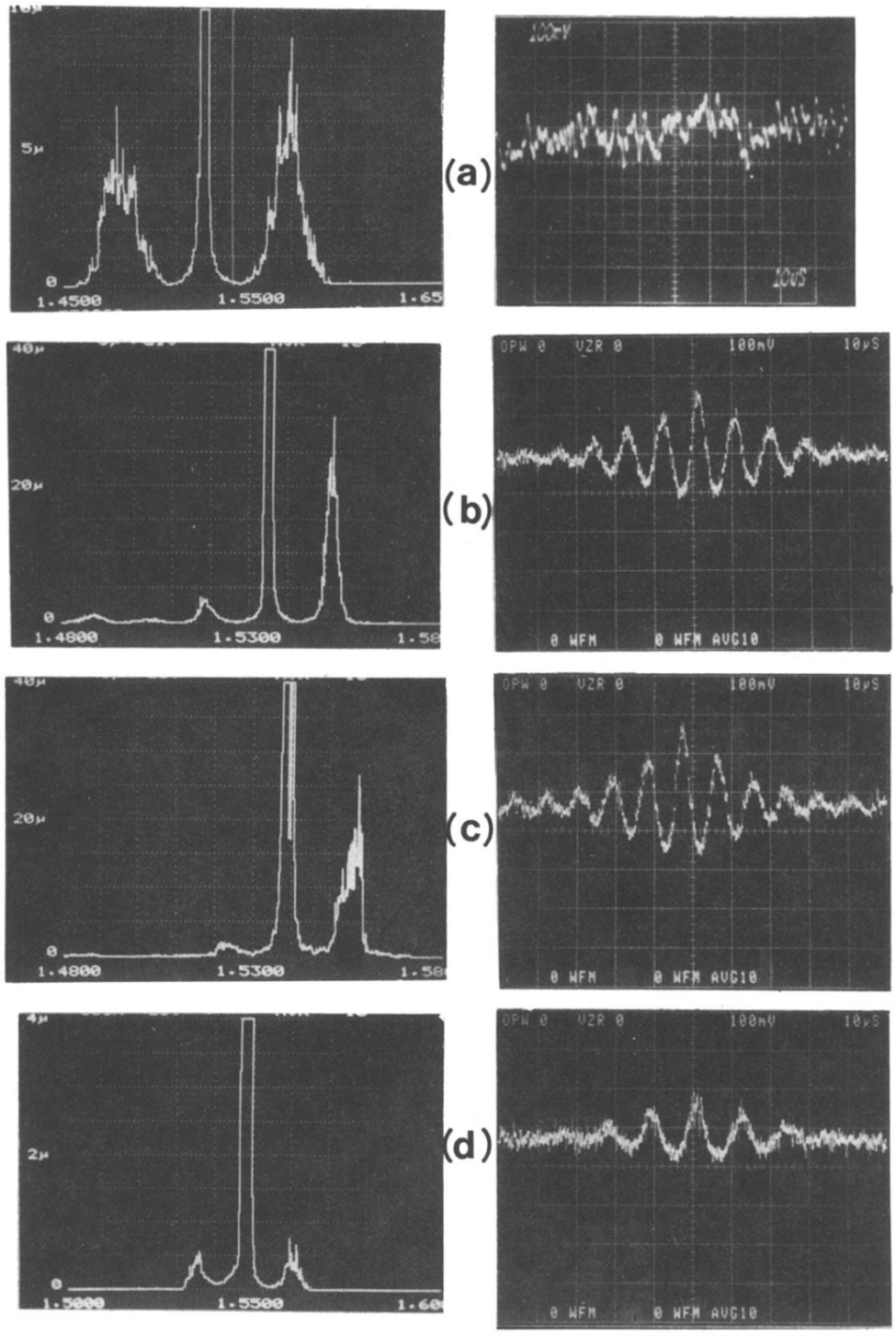

FIG. 2. Pump-wavelength dependence the oscillation waveforms and spectra of the MIO. (a)–(d) correspond to pump wavelengths of 1.525, 1.535, 1.540, and 1.550 μm, respectively. Spectra are on the left-hand side and the corresponding autocorrelation waveforms are on the right-hand side. One division of the autocorrelation waveforms corresponds to 0.5 ps.